

AperTO - Archivio Istituzionale Open Access dell'Università di Torino

**New Formulation of Functionalized Bioactive Glasses to Be Used as Carriers for the Development of pH-Stimuli Responsive Biomaterials for Bone Diseases**

**This is the author's manuscript**

*Original Citation:*

*Availability:*

This version is available <http://hdl.handle.net/2318/143640> since 2015-12-30T18:14:05Z

*Published version:*

DOI:10.1021/la5003989

*Terms of use:*

Open Access

Anyone can freely access the full text of works made available as "Open Access". Works made available under a Creative Commons license can be used according to the terms and conditions of said license. Use of all other works requires consent of the right holder (author or publisher) if not exempted from copyright protection by the applicable law.

(Article begins on next page)



UNIVERSITÀ DEGLI STUDI DI TORINO

This is an author version of the contribution published on:

Valentina Aina, Claudio Magistris, Giuseppina Cerrato, Gianmario Martra,  
Guido Viscardi, Gigliola Lusvardi, Gianluca Malavasi, Ledi Menabue  
New Formulation of Functionalized Bioactive Glasses to Be Used as Carriers  
for the Development of pH-Stimuli Responsive Biomaterials for Bone  
Diseases

LANGMUIR (2014) -  
DOI: 10.1021/la5003989

The definitive version is available at:

<http://pubs.acs.org/doi/abs/10.1021/la5003989>

# New formulation of functionalized bioactive glasses to be used as carriers for the development of a pH- stimuli responsive biomaterials for bone diseases

*Valentina Aina,<sup>\*a</sup> Claudio Magistris,<sup>a</sup> Giuseppina Cerrato,<sup>a</sup> Gianmario Martra,<sup>a</sup> Guido Viscardi,<sup>a</sup>  
5 *Gigliola Lusvardi,<sup>b</sup> Gianluca Malavasi,<sup>b</sup> and Ledi Menabue<sup>b</sup>**

<sup>a</sup> Department of Chemistry, Centre of Excellence NIS (Nanostructured Interfaces and Surfaces);  
INSTM (Italian National Consortium for Materials Science and Technology), University of Torino,  
Via P. Giuria 7, 10125 Torino, Italy. ; **E-mail: valentina.aina@unito.it**

<sup>b</sup> Department of Chemical and Geological Science, University of Modena and Reggio Emilia, Via  
10 Campi 183, 41125 Modena, Italy.

**KEYWORDS:** Smart drug delivery systems (DDS); Stimuli-responsive biomaterials; bioactive  
glasses; pH-sensitive linker.

## ABSTRACT:

The aim of the present contribution is to prepare a functionalized bioactive glass potentially useful as prosthetic material, but also able to release organic molecules in response to a change of the pH environment. By this approach it is possible to develop devices which can be used for a triggered drug release in response to specific stimuli; this is an attractive research field, in order to avoid either systemic and/or local toxic effects of drugs. In particular, in the present paper we report data related to the development of a new formulation of bioactive glasses, their functionalization with organic molecules to obtain a pH-sensitive bond, their physico-chemical characterization and in-vitro bioactivity in simulated biological fluids (SBF) and organic molecules delivery tests at different pH. The glass functionalization, by means of a covalent reaction, allows to produce a model of pH-responsive bioactive biomaterial: when it is exposed to specific pH changes, it can favour the release of the organic molecules directly at the target site. Cysteamine and 5-aminofluorescein are used as model molecules to simulate a drug. The materials, before and after the different functionalization steps and in-vitro release tests at different pH, have been characterized by means of different experimental techniques such as: X-ray Powder Diffraction (XRPD), Raman, ~~and~~ FTIR and Fluorescence spectroscopies, N<sub>2</sub> adsorption, thermogravimetric (TGA) and Elemental Analysis.

## INTRODUCTION

Bone defects can be generated by a variety of diseases or traumatic injuries, such as tumor resection, periodontal resorption, congenital defects, and arthroplasty revision surgery.<sup>1,2</sup> Bioactive glasses and glass-ceramics represent a class of materials, that, due to their tailorable properties, can be used to treat bone defects.<sup>3,4</sup> Recently, new therapeutic strategies using synthetic biomaterials as carrier for drugs and biological molecules have been developed.<sup>5-7</sup> Controlled drug delivery systems have already made an enormous impact on the medical field with a million patients a year using a form of controlled release system or another. Despite the success of controlled release systems there are still significant challenges remaining to make next generation drug delivery systems that can target and respond to specific diseases conditions. The development of intelligent therapeutic and systems has transformed the research field of controlled drug delivery, tissue engineering, and biosensors.<sup>1</sup>

More importantly, these devices will be “intelligent” and will release the drug when the patient is in need of its therapeutic effects.<sup>5</sup> Micro- and nano-scale intelligent systems can maximize the efficacy of therapeutic treatments because they have the ability to rapidly detect and respond to disease states directly at the local site. To this purpose micro- and nanotechnologies can offer new opportunities towards the development of better, intelligent medical systems and devices that have the possibility to profoundly impact medical therapeutic techniques. Cell-cell and cell biomaterial interactions are microscale events.<sup>8</sup> The development of devices that will interact with cells on the micro level will potentially target and treat the problem and, at the same time, alleviate extreme damage to entire tissues or even organs reducing the inflammatory response.<sup>5,9</sup> The development of devices to be used for a triggered release of drug directly at the tumor sites represents an attractive research field in order to avoid the toxic effects of anti-cancer drugs. Despite advances in the development of new anti-tumor drugs, these drugs still possess significant serious side effects that limit the dose size as well as the use of the drugs. In this way it is possible to obtain a high local dose in tumor sites and less side effects, this is a very desirable property in carrier designs for tumor chemotherapy.<sup>10</sup>

Approaches to achieve triggering systems include magnetic,<sup>11</sup> thermal<sup>12</sup> and ultrasonic activation<sup>13</sup> for enhanced drug release from the carriers, which were specifically designed to respond to external signals or energy. The external activation could be useful for the tumors whose location is well-identified and which are accessible by external signal or energy sources. In addition it would be difficult to restrict the activation only on tumor regions and thus the external activation does not distinguish the blood compartment and tumor cells. The difference of pH between solid tumors and normal tissue has been long recognized. For instance, the average extracellular pH values of human solid tumors fall below 7.0. The difference of pH is small but it represents a natural signal of solid tumors for triggered release. Some approaches have described drug release by cleavages of chemical bonds, which conjugate a drug to polymers.<sup>14,15</sup> **By exploiting bioactive glasses, it is possible to combine** the ability of these materials to restore bone defects and at the same time, to release under controlled conditions, biological molecules immobilized onto/into the materials. The covalent attachment of functional organosilanes to silica and glass substrates has proven to be an efficient means of immobilizing antibodies and cellular receptors as well as DNA array or drugs. Due to the presence of silanols groups exposed on glasses surface, under controlled conditions, it is possible to bond biomolecules on the glasses surfaces; Vernè et al.<sup>16</sup> optimized a procedure to functionalize glasses surface with 3-amino-propyl-triethoxysilane (APTS) in order to exploit the presence of amino groups to bind proteins.<sup>17</sup> The disadvantage of this procedure is the low **amount and** stability of grafted APTS molecules that can be partially removed from glass surface during the immobilization with proteins or drugs. In the present paper, in order to increase the **amount and** stability of APTS molecules grafted onto the glasses surface, a series of amino-propyl **sol-gel** bioactive glasses (APTS**BSG**) have been prepared and thoroughly characterized. **Moreover,** the HA/HCA formation has been evaluated by means of in-vitro bioactivity tests. APTS molecules have been inserted during the glasses synthesis procedure **where they have been partially or totally substituted for** tetraethyl orthosilicate (TEOS) molecules commonly used as SiO<sub>2</sub> sources for the glasses' preparation. In order

to define the best conditions to obtain a new type of APTS-containing bioactive glasses all the as-synthesized materials have been characterized with different experimental techniques. It has been verified that APTS molecules are firmly anchored into the glass structure. Although other authors<sup>18</sup> report the preparation of silica network using both TEOS and APTS, to the best of our knowledge this is the first study in which APTS has been inserted during the sol-gel synthesis of a bioactive material having an high concentration of amino groups firmly anchored to the glasses surface. In order to develop a pH-sensitive bioactive glass the APTSBSG glass exhibiting the best chemical and morphological biological properties, developed in the present work, has been functionalized by means of a covalent reaction to produce a pH-responsive bioactive biomaterial which, when exposed to specific pH changes, it can favour the drug release at the target site.

To this purpose, the glass exhibiting the best chemical and morphological properties (indicated in the paper as APTS25SG432) was first functionalized with maleic and cis-aconitic anhydrides, among the most common pH sensitive spacers.<sup>19</sup> Cysteamine and 5-aminofluorescein, chosen as simple and non toxic models to simulate a drug, were then conjugated to the maleilated bioglass. Finally, In-vitro delivery tests at different pH values have been were then performed in order to observe the effective release of the pH dependent covalent bond.

In particular, the use of cysteamine allowed to detect the presence of sulphur in the conjugate by Elemental Analysis; the conjugation with 5-aminofluorescein made it possible to determine quantitatively the fluorophore release in solutions.

## EXPERIMENTAL

### Materials

*Reference and APTS containing glasses.* In order to obtain a series of sol-gel amino-propyl bioactive glasses the conventional SiO<sub>2</sub> source (tetraethyl orthosilicate, TEOS) was partially or totally substituted with 3-aminopropyltriethoxysilane (APTS). The samples are referred as APTS<sub>xx</sub>SG<sub>yyy</sub>, where xx is the percentage of APTS used as precursor of SiO<sub>2</sub> (xx = 25, 50 and 100) and yyy is the temperature of the thermal treatments (yyy = 423K).

In **Table 1** the theoretical compositions, in molar %, and the thermal treatments of the studied samples are reported.

-----  
(Please, insert here **Table 1**)  
-----

The glass samples with theoretical molar composition 15CaO·5P<sub>2</sub>O<sub>5</sub>·80SiO<sub>2</sub> were synthesized using a sol-gel route as reported in our previous papers.<sup>20,21</sup> The samples were prepared using an appropriate mixture of tetraethylorthosilicate (TEOS) and 3-aminopropyltriethoxysilane (APTS) as SiO<sub>2</sub> source, triethylphosphate (TEP) and calcium nitrate tetrahydrate (Ca(NO<sub>3</sub>)<sub>2</sub>·4H<sub>2</sub>O) have been used as P<sub>2</sub>O<sub>5</sub> and CaO sources, respectively. A water solution was prepared dissolving specific amounts of Ca(NO<sub>3</sub>)<sub>2</sub>·4H<sub>2</sub>O in a mixture of 0.2 ml HCl (37% w/w) and 5.0 ml of H<sub>2</sub>O. This aqueous solution was added to 40 ml of ethanol where different amount of TEOS and APTS were mixed in order to obtain the different APTS/TEOS ratios. TEP has been previously added to each APTS/TEOS mixture (each addition every 3 hours), in order to obtain the stoichiometric compositions. The solutions were then stirred for 1 hour and cast in Teflon<sup>®</sup> containers, that were hermetically closed and kept 1 day at room temperature for gelation. Gels were then aged 1 day at 333K.

The aged systems were treated at 423K for 3 hours in an open Al<sub>2</sub>O<sub>3</sub> crucible (heating ramp: 2°C/min); the latter temperature value has been chosen on the basis of the thermogravimetric analyses performed

on the APTS containing samples. This is the highest calcination temperature to be used in order to avoid the decomposition of the  $-\text{CH}_2-\text{CH}_2-\text{CH}_2-\text{NH}_2$  chains of APTS molecules inserted during the synthesis.

Finally, the obtained powders were grounded manually in an agate mortar for 5 minutes and sieved in order to obtain powders of  $\text{Ø} < 500\mu\text{m}$ . The grinding process was not performed on the APTS100SG423 (samples with the highest amount of APTS) due to their sticky consistency.

In order to remove the nitrate still present in the samples, the powders of SG423, APTS25SG423 and APTS50SG423 glasses have been washed with a solution of  $\text{Ca}(\text{OH})_2$  0.1M for 1 hour under magnetic stirring. The powders were then filtered and re-dried at 423K for 3 hours in an open  $\text{Al}_2\text{O}_3$  crucible (heating ramp:  $2^\circ\text{C}/\text{min}$ ) and grounded again in an agate mortar for 5 minutes and sieved in order to obtain powders of  $\text{Ø} < 500\mu\text{m}$ . The Elemental Analysis performed on APTS25SG423 sample before the washing procedure evidenced that the percentage of N is 7.5%. Based on stoichiometric, the percentage of N in the material should be  $\sim 8.6\%$ ; this value is the sum of N derived by  $-\text{NH}_2$  groups of APTS (4.9%) and from  $\text{NO}_3^-$  groups of calcium nitrate (3.7%). After washing, the amount of N decreased to 5.8%. This datum suggest a drastic reduction of nitrates in the material; the N still present in the material is mainly due to  $-\text{NH}_2$  groups of APTS. Moreover, in order to completely remove N deriving from nitrates, others attempts were performed using other calcium sources; such as  $\text{Ca}(\text{CH}_3\text{COO})_2$  and  $\text{CaCl}_2$ . Concerning acetate it strongly interacts with  $-\text{NH}_2$  groups preventing the following functionalization step, whereas in the case of calcium chloride the amount of residual chlorine after the washing procedure was higher with respect to that of nitrates. The toxicity of nitrates is well known<sup>22</sup> however in view of a potential application of these materials the washing showed a drastic reduction of these species. Accurate washing steps allow to remove completely nitrates species but this is not strictly concerning with this study.

After the thermal treatments and the sample washing, the compositions were again verified by Elemental Analysis in order to evaluate the amount of C and N. The amount of C and N was described

in the results and discussion section; concerning SG423, APTS25SG423 and APTS50SG423 samples. The experimental compositions of samples were determined by EDS analysis and are reported in **Table 2** (expressed as oxides molar percentage). ~~has been carried out in order to evaluate the nominal composition of the system 15CaO-5P<sub>2</sub>O<sub>5</sub>-80SiO<sub>2</sub>.~~

5

-----  
(Please, insert here **Table 2**)  
-----

The experimental compositions differ from the theoretical one slightly by the lower amount of CaO and higher % of SiO<sub>2</sub>. This can be due to the washing step that causes the release of calcium.

10 The two reference samples prepared with only TEOS as precursor of SiO<sub>2</sub> were then treated at 423 or 873K for 2 hours to stabilize the glass system (elimination of solvents and reagents residues). The samples are referred to in the following as SG423 and SG873, respectively. The powders obtained were grounded with the same procedure performed on APTSxxSGyyy samples.

*Post-synthesis functionalization with APTS.* In order to introduce -NH<sub>2</sub> groups in potential bioactive 15 glass samples avoiding the presence of residues derived from synthesis precursors (*i.e.* nitrates species), a post synthesis surface functionalization with APTS has been also carried out on the SG873 sample; this sample is referred as SG873psAPTS. For the preparation of this sample, 1 g of SG873 powder was soaked for 2 hours in 40 ml ethanol solution where previously 1 ml of APTS and 0.5 ml of a 10% HCl solution were dissolved. The powder has been filtered and dried at 423K for 3 hours in an 20 open Al<sub>2</sub>O<sub>3</sub> crucible (heating ramp: 2°C/min). As previously mentioned in the introduction section, the material with the best chemical and morphological properties has been conjugated with a suitable organic molecule by means of a pH-sensitive covalent bridge.

*Preparation of maleilated bioactive glass and conjugation with Cysteamine.* α,β-Unsaturated dicarboxylic acid anhydrides, such as maleic or cis-acetic anhydrides, have been used as acid- 25 sensitive spacers between drugs and carriers, because they are able to release an active drug from the

carrier into a tumor tissue, either in slightly acidic extracellular fluids or, after endocytosis, in endosomes or lysosomes of cancer cells.<sup>23</sup> **With To** this purpose **in-mind**, the APTS25SG423 glass was first reacted with maleic or cis-aconitic anhydride; the vinyl carboxyl group of the resulting maleilated bioactive glass was then reacted with the amino group of a target molecule, in order to obtain the desired conjugate. Reaction conditions for the synthesis of maleamic acids from alkylamines and maleic anhydride were successfully applied in the functionalization of APTS25SG423.<sup>24</sup> In a model reaction with pentylamine, **mass spectrometry – electrospray ionization (MS-ESI)** analysis confirmed the formation of maleic acid N-pentylmonoamide, in which the free carboxyl group represents a useful functionality for binding a suitable drug. (Model reaction scheme is reported in the supplementary materials, Scheme 1 SM) Scheme 1 **section A** reports the synthesis of the vinyl carboxyl acid on the bioglass surface. The **potential** of the functionalized bioactive glass as pH-sensitive bridge in drug delivery was then evaluated. To this purpose cysteamine (2-aminoethanethiol, **TEA**) and **5-aminofluorescein** were chosen as a simple and non-toxic models and **they were** conjugated with the modified bioactive glass, by activation of the vinyl carboxylic acid with the established **1-Ethyl-3-(3-dimethylaminopropyl)-carbodiimide (EDC), N-hydroxysuccinimide (NHS)** protocol. In **Scheme 1 section B and C** report the conjugation with cysteamine and **5-aminofluorescein, respectively.**

-----  
(Please, insert here **Scheme 1**)  
-----

<sup>20</sup> The amount of NH<sub>2</sub> groups available at the **APTS25SG423** glass surface, determined by acid-basic titration, is 3.5 mmol/g (0.09 mmol/m<sup>2</sup>).

*Synthesis of APTS25SG423-MA.* 0.30 g of APTS25SG423 glass (1.05 mmol NH<sub>2</sub>) and 0.10 g of maleic anhydride (1.05 mmol) and 10 mL anhydrous diethyl ether were introduced in a round bottom flask, previously dried in oven and flushed with Ar; the suspension was let under stirring at room

temperature for 5 min, then filtered on Büchner funnel and washed with acetone, yielding 0.22 g of APTS25SG423-MA.

The same procedure was applied to cis-aconitic anhydride, yielding 0.24 g of APTS25SG423-CAA.

The amount of  $\text{NH}_2$  groups available at the glass surface after reaction with maleic anhydride, determined by acid-basic titration, is 0.9 mmol/g (0.02 mmol/m<sup>2</sup>). This datum indicates that the degree of substitution is ~75%. In order to avoid the glass degradation it was not possible to increase the reaction time.

*Conjugation of APTS25SG423-MA with Cysteamine.* 0.85 g of maleilated APTS25SG423 (0.85 g, 2.2 mmol -COOH), 1.69 g of 1-Ethyl-3-(3-dimethylaminopropyl) carbodiimide hydrochloride (8.8 mmol), 1.01 g N-Hydroxysuccinimide (8.8 mmol) and 40 ml anhydrous Dimethyl Sulfoxide (DMSO) were introduced in a round bottom flask, previously dried in oven and flushed with Ar, and let under stirring for 30 min at room temperature in dark, giving a yellow solution; cysteamine hydrochloride (0.25 g, 2.2 mmol) and triethylamine (0.22 g, 2.2 mmol) were then dissolved in anh. DMSO, flushed with Ar and added dropwise to the previous solution; the mixture was let under stirring in dark at room temperature for 1 hour, then filtered on a Büchner funnel and washed with DMSO and acetone, affording 0.77 g of APTS25SG423-MA-CYST conjugate. ~~In order to verify if the two synthesis procedures have been carried out with success, the samples have been analysed by means of Raman spectroscopy and elemental analysis.~~

*Conjugation of APTS25SG423-MA with 5-aminofluorescein.* 1.47 g of maleilated APTS25SG423 (3.8 mmol -COOH), 2.91 g of 1-ethyl-3-(3-dimethylaminopropyl) carbodiimide hydrochloride (15.2 mmol), 1.75 g N-hydroxysuccinimide (15.2 mmol) and 110 ml anhydrous DMSO were introduced in a round bottom flask, previously dried in oven and flushed with Ar, and let under stirring for 30 min at room temperature in dark; 5-aminofluorescein (1.33 g, 3.8 mmol) was then dissolved in 30 mL of DMSO and flushed with Ar; the orange solution was added dropwise to the glass suspension, and the

mixture was let under stirring at room temperature in dark for 1 hour, then filtered on a Büchner funnel and washed with DMSO and acetone, giving 1.35 g of APTS25SG423-MA-AF conjugate.

In order to verify if the synthetic procedures had been carried out with success, the samples were analysed by means of Raman spectroscopy and elemental analysis.

5

## Methods

### *Materials characterization*

*Scanning electron microscopy (SEM)*. SEM microscopy was used to investigate any effect of the addition of different amounts of APTS on the morphology of bioactive glasses and the EDS analysis were done to determine the experimental compositions of the prepared samples. Moreover, the morphology of the samples were investigated after 14 days of SBF soaking and Energy-dispersive X-ray spectroscopy (EDS) was performed in order to control the composition of the sample surfaces. The images were obtained with a ZEISS ECO 50 XVP microscope equipped with a LaB<sub>6</sub> source, with acquisition of images at 15 kV. For each sample, four different sample areas were investigated. XRPD (*X-Ray Powder Diffraction*). XRPD (*X-Ray Powders Diffraction*) patterns were recorded on a PANalytical X'Pert Pro Bragg-Brentano diffractometer, using Ni-filtered Cu K $\alpha$  radiation ( $\lambda = 1.54060 \text{ \AA}$ ) with X'Celerator detector. The patterns were taken over the diffraction angle  $2\theta$  in the 10-50° range, with a time step of 50 s and a step size of 0.03°.

*Specific surface area and porosity measurements (N<sub>2</sub> or Kr adsorption at 77K)*. Specific surface area (SSA) and porosity were evaluated by adsorption of an inert gas (N<sub>2</sub>) at the temperature of liquid nitrogen (77K) using a Micromeritics ASAP 2020 porosimeter. In the case of samples with very low SSA, Kr was used as adsorptive gas.

For specific surface area determination data were analyzed with the BET model<sup>25</sup> BJH<sup>26</sup> model was used to analyze mesopores, and 't-plot' (statistical thickness method)<sup>27</sup> was employed to evaluate the presence of micropores. The accuracy of BET model for SSA determination is known to be per se

25

relatively low (~ 5%), whereas both instrumental accuracy and reproducibility of data obtained with modern automatic gas-volumetric instrumentation are quite high. For a review on those methods, see Gregg and Sing.<sup>28</sup>

Before the measurements, the samples were outgassed at room temperature (RT) for 12 hours under vacuum (~ 10<sup>-5</sup> Torr).

*Thermogravimetric analyses and differential thermal calorimetry (TGA-DSC).* The stability of the materials was investigated by thermo gravimetric analyses coupled with differential thermal calorimetry under N<sub>2</sub> flow (ramp: 10 °C min<sup>-1</sup>) by a TA instrument Q600 SDT Simultaneous DSC-TGA heat flow analyser.

*Raman spectroscopy.* FT-Raman spectra were collected directly on the glass powders in the 4000-100 cm<sup>-1</sup> range. A Bruker Vertex 70 instrument with the RAM II accessory, equipped with NdYAG laser (1064 nm) was used: 15000 scans with a mean laser power of 50 mW were accumulated for each sample.

*Infrared spectroscopy.* KBr pellets: KBr pellets of samples as synthesized were prepared by mixing ~1 mg of powder with ~ 50 mg of specpure KBr. Transmission spectra of KBr pellets were normally recorded using a DTGS detector in order to inspect also the low-ν region of the 4000-400 cm<sup>-1</sup> spectral range and performing 128 scans for each measurement.

Pure pellets: IR spectra of the pure pellets (self supported pellets, ~ 10 mg·cm<sup>-2</sup>) of synthesized systems were collected. Each sample was activated in vacuo at different temperatures to investigate both nature/structure and thermal stability of the solid surface terminations.

*Fluorescence spectroscopy.* All measurements were performed using a JASCO FP6200 fluorescence spectrophotometer. The slits were adjusted to achieve a spectral bandwidth of 2 nm, and the spectra were obtained with a 1 nm step size and 1 s integration time. The samples were excited at a wavelength of 490 nm. The standards of 5-aminofluorescein were prepared in the concentration range between 10<sup>-5</sup>-10<sup>-7</sup> M, because in this range the intensity of the fluorescence band at 510 nm was

proportional to the concentration (Abs in the range 0.1-0.2). As fluorescence properties of the 5-aminofluorescein are strictly pH-dependent, before the measurements the pH of both standard and samples solutions was adjusted to pH ~ 7.4 using phosphate buffered solution (PBS).

*Mass Spectrometry.* Mass spectra were recorded with a Thermo Finnigan Advantage Max Ion Trap Spectrometer, equipped with an electrospray ion source (ESI) in either positive or negative ion acquiring mode.

*Acid-base titration.* Acid-base titration was conducted by suspending the sample (50 mg) in 10 ml of HCl solution (0.1M) for 1 hour. Then, the solution was centrifuged to remove glass powder and 4 ml of the acid solution (after the glass contact) were are titrated with NaOH solution (0.1M) using phenolphthalein as indicator. Data were a mean of three independent determinations on different samples.

*Elemental analysis.* Elemental analysis was conducted with a Perkin Elmer 2400 NCHS analyzer before and after the washing procedure and after each functionalization step, to determine the successful functionalization of the materials. Data were a mean of three independent determinations on different samples.

*In-vitro bioactivity tests.* In order to monitor the bioactivity of sol-gel amino-propyl bioactive glasses (APTSxxSGyyy), we used the simulated body fluid (SBF) proposed by Kokubo et al.<sup>29</sup> SBF is an acellular aqueous solution with an inorganic ion composition almost equal to human plasma. The bioactivity response of the materials was evaluated in terms of the formation of a HA/HCA layer on the surface of 250 mg of powdery samples after being soaked in 50 mL of SBF at different times (1, 2, 4 and 8 hours and 1, 4, 7 and 14 days). Furthermore, in vitro studies allowed us to compare the relative kinetics of the bioactive response for different samples: the shorter the time required for the HA/HCA layer formation, the higher the bioactivity of the material. The HA and/or HCA formation on the surface of the glasses was monitored by XRD diffraction, SEM-EDS and FT-IR spectroscopy. In

parallel, the chemical composition of the supernatant solution was monitored by inductively coupled plasma emission spectroscopy (ICP-ES) analysis and pH determination.

*Inductively coupled plasma emission spectroscopy (ICP-ES) analysis.* Changes in the concentrations of calcium, silicon and phosphorous in the solutions were measured on an ICP spectrometer (ICP Optima 4200DV, Perkin Elmer) at every leaching time mentioned above. The concentrations reported represent the mean value of three different determinations on the same sample solution.

*pH-dependent release tests.* In order to evaluate the bond stability at different pH values 10 mg of APTS25SG423-MA-CYST and APTS25SG423-MA-AF conjugates were soaked in 2 ml of buffered solution for 1 and 72 hours. The buffered solutions used were two: *i*) buffer at pH = 4.5 (acetic/acetate buffer); *ii*) buffer at pH = 7.4 (PBS buffer). After different soaking times, the powders were separated from the solution by filtration. ~~dried at 423K and analysed by Raman spectroscopy~~ In the case of cysteamine conjugate the powders were analyzed by Raman spectroscopy whereas for the 5-aminofluorescein conjugate the amount of aminofluorescein in the solutions was determined by fluorescence spectroscopy.

## RESULTS AND DISCUSSION

In the present **paper**, the synthetic procedure of sol-gel amino-propyl bioactive glasses (APTS<sub>xx</sub>SG<sub>yyy</sub>) was optimized. The material, exhibiting the ~~best-chemical-and-biological~~ **most promising chemical and morphological** properties, has been conjugated with maleic and cis-aconitic anhydrides in order to obtain an acid-sensitive bond. This bond ~~was then will-be~~ exploited to obtain a controlled drug release stimuli-responsive biomaterial.

*Materials characterization.* In **Figure 1** SEM micrographs of the investigated samples are reported.

-----  
(Please, insert here **Figure 1**)  
-----

10

For all samples the morphology is quite irregular. The morphology of both reference glasses is similar: for sake of brevity only SEM micrographs of SG873, APTS25SG423, APTS50SG423 and APTS100SG423 ~~has~~ **have** been reported. The **aggregate** size is influenced by **the grinding procedure and** the amount of APTS introduced during the synthesis procedure. In the case of the reference glasses (Section A) the **aggregate** shape is rectangular with a particle size in the 100-300  $\mu\text{m}$  range and each particle presents many cracks. As a consequence of the introduction of a small amount of APTS during the synthesis procedure (APTS25SG423, Section B) the glass morphology is evidently modified. The **aggregate** sizes decreased in the 10-30  $\mu\text{m}$  range **probably due to the fragility of the sample during the grinding procedure** and now the particles being roundish. Increasing the amount of APTS in the glass composition (APTS50SG423, Section C) the particles size **became quite** mixed: both small aggregated particles with 10-30  $\mu\text{m}$  dimensions and particles with a size in the 100-300  $\mu\text{m}$  range, the latter being very similar of these of reference glass (SG873) in term of size, but exhibiting a more roundish aspect, most likely due to the presence of APTS. Finally, in the case of APTS100SG423 (Section D) sample (all TEOS has been replaced by APTS during the synthesis), the particles sizes increased **till** 300-500  $\mu\text{m}$  in fact, **during the grinding procedure the material was very**

15  
20  
25

sticky, their shape became rectangular and on top of them it is possible to observe the presence of small aggregates probably made up of APTS. As a consequence of the large amount of organic chains (-CH<sub>2</sub>-CH<sub>2</sub>-CH<sub>2</sub>-NH<sub>2</sub>), the APTS100SG423 sample is not very powdery but rather sticky: for this reason it is difficult to ground it after the synthesis. The morphology of this sample is characterized by the presence of large aggregates ~~and these aggregates~~, which in turn can include smaller ones. The morphology of the SG873psAPTS sample (reference glass functionalized post-synthesis with APTS) is similar to that of SG873 sample (Section A): for this reason, it has not been reported in a specific figure. XRD patterns obtained for the as-synthesized samples evidenced the typical halo of a glass with the maximum in the range between 20-25° in °2θ, characteristic of amorphous systems. (see **Figure 1 SM**) Specific surface area and porosity data of as-prepared samples are reported in **Table 3**.

-----  
(Please, insert here **Table 3**)  
-----

The two reference samples possess a high specific surface area typical of sol-gel glasses. In particular, the sample that has been thermally treated post-synthesis at low temperature 423K namely, SG423 exhibits a SSA of ~ 147 m<sup>2</sup>/g, no microporosity but only mesoporosity with an average pores width of ~ 26Å and mesopores area of ~ 120 m<sup>2</sup>/g. Concerning the reference sample thermally treated at higher temperature, 873 K namely, SG873 the SSA increases at ~ 258 m<sup>2</sup>/g, whereas mesopores area and width remains almost unchanged with respect to SG423 sample. Conversely, this sample presents microporosity, with micropore area of ~ 95 m<sup>2</sup>/g. With the introduction of increasing amount of APTS instead of TEOS, the SSA significantly decreases; in the case of APTS25SG423 sample, the SSA becomes lower (~ 38 m<sup>2</sup>/g), becoming for APTS50SG423 and APTS100SG423 samples, ~ 15 and ~ 3 m<sup>2</sup>/g, respectively. This can be explained by the high % of organic chains (-CH<sub>2</sub>-CH<sub>2</sub>-CH<sub>2</sub>-NH<sub>2</sub>) presenting in APTS-rich samples: the glass matrix made of APTS molecules could strongly interact with ethanol, formed during the hydrolysis and condensations steps, and these residues are not

completely removed during the post-synthesis thermal treatment at 423K. For this reason the formation of fine powders and pores typical of a dried gel is inhibited. These results are in good agreement with the data reported in our previous work,<sup>21</sup> in which the characterization by SEM microscopy of SG423 sample evidenced the presence of fine granules (20-30  $\mu\text{m}$  of mean dimension) with pores that were due to the elimination of the organic residues formed during the sol-gel process.

In **Figure 2** the results obtained by means of thermo gravimetric analyses (TGA) are reported.

-----  
(Please, insert here **Figure 2**)  
-----

Section A of Figure 2 reports data indicated as percentage of weight loss vs. temperature (K), whereas Section B shows data as weight derivative (%/K) vs. temperature (K). The thermograms of Figure 2 section A and its derivatives (section B) evidenced that the percentage of mass loss as a function of the temperature can be divided in different ranges, most likely corresponding to different processes. The events that occur can be summarized as follows:

- i*) in the 323-423K range, there is the first weight loss mainly due to the loss of physisorbed water; in fact, in the plot of weight derivative (%/K) vs. temperature (K) the maximum is centered at  $\sim 373\text{K}$ ;
- ii*) the second event, in the 423-523K temperature range, can be due a) in part to the elimination of APTS molecules and/or hydrolysed APTS molecules not condensed with the silica glass matrix and b) in part to the organic residues derived by TEOS and TEP molecules. This is in agreement with the boiling temperature of APTS molecules (493K); note that the plain SG873 sample exhibits no mass loss in this temperature range, as it contains no extra species (APTS);
- iii*) the third process takes part between 523 and 673K: it is likely to be due to the decomposition of organic chains derived by hydrolysed and condensed APTS molecules into the glass matrix. In the case of the post-synthesis functionalized sample, SG873psAPTS (B) this weight loss is centred at 543K, whereas in the case of APTS25SG423 (b), APTS50SG423 (c), and APTS100SG423 (d) glasses the

weight losses are centred at 593, 603 and 613K, respectively. Moreover, increasing the amount of APTS the percentage of weight loss in this range increased. The reference SG873 glass exhibits no weight loss in this range. These results put in evidence that, when APTS molecules are condensed on the glass surface (SG873psAPTS sample), the decomposition temperature of the organic chain deriving from APTS is lower than that of the condensed APTS molecules (APTSxxSGyyy samples). In the case of post synthesis functionalization, the glass surface rich of hydroxyl groups (*i.e.*  $\equiv\text{Si-OH}$ ) reacts with APTS molecules that are bounded only onto the glass surface. On the other hand, in the case of APTSxxSGyyy samples the organic chain derived by APTS are uniformly distributed in the bulk glass structure and they are strongly bonded to the amorphous glassy matrix: thus, this increases the decomposition temperature of the APTS organic chain. Concerning the SG473 sample, in this temperature range it exhibits a small mass loss, which is due only to the decomposition of the nitrate residues that are still present in the glasses;

*iv*) in the 673-923K range, there is the last weigh loss most likely due to the removal of all residual species deriving from synthesis precursors. Concerning the samples treated at 873K, no weight loss is observed in this temperature range because all the residual species have been already removed during the post-synthesis thermal treatments at 873K. **Interesting to note that in the 773-873K range the nitrate residues should be eliminated: for the APTS100SG423 the mass loss is around 6%, while for APTS50SG423, APTS25SG423 and SG423 is lower than 2% confirming that the washing procedure performed only on APTS50SG423, APTS25SG423 and SG423 was able to eliminate a great amount of nitrate, while the sample APTS100SG423 that was not washed the elimination of nitrate during TGA was more evident.**

**Figure 3** reports Raman spectra collected onto as-synthesized samples.

-----  
(Please, insert here **Figure 3**)  
-----

By the inspection of Raman spectra the following features can be evidenced:

- i) the bands at  $\sim 2960$  and  $\sim 2940 \text{ cm}^{-1}$ , typical of asymmetric and symmetric C-H stretching vibrations, are present in all 423K calcined samples: these bands are due to the presence of APTS molecules and organic residues used during the glasses synthesis. The intensity of these bands increases with increasing the amount of APTS in the glasses composition. Moreover, in the case of APTS-containing samples (spectra b, c and d) the intensity ratio between these bands is similar to that observed in the case of pure APTS (spectrum 1, reported as a reference);
- ii) the bands at  $\sim 1450$  and  $1200 \text{ cm}^{-1}$  are characteristic of C-H bending modes (counter parts of the bands described in (i));
- iii) the sharp band at  $\sim 1040 \text{ cm}^{-1}$  is typical of carbonate species; this is present only on the samples calcined at 423K; the highest calcination temperature (823K) removed all the carbonate species (see spectra A and B).

FTIR spectra confirm the same features already reported in the case of Raman spectra; for sake of brevity FTIR spectra are reported in the supplementary material. (see **Figure 2 SM**).

From this morphological and physico-chemical characterization study, among all synthesized samples, the sample **APTS25BSG423** shows the best compromise between morphological and surface properties.

For this reason, the sample **APTS25BSG423** has been chosen to be deeply investigated; in particular the bioactivity in simulated body fluid (SBF) of this sample in comparison with the two reference glasses has been evaluated.

*In-vitro bioactivity tests.* The bioactivity in simulated biological fluid (SBF), according to the Kokubo's recipe<sup>29</sup> has been carried out on the **APTS25SG423**, **APTS50SG423** and **SG873psAPTS glasses** in comparison with the two reference glasses SG423 and SG873. This experiment has the aim to evaluate the effect of the introduction of the APTS in the glass synthesis on the bioactivity.

There is a well-established relationship between the ability of a given material to form bonds with living tissues and its ability to grow an apatite-like layer when soaked in fluids mimicking human plasma, and for this reason, in vitro assays are common and widely employed tools in the bioactivity study of new candidate implant materials. The bioactivity response of the materials were evaluated in terms of the formation of a HA/HCA layer on the surface of powdery samples after being soaked in SBF at different times (1, 7 and 15 days). The materials resulting coated by a HA/HCA layer were considered bioactive, whereas if the glass surface remained unchanged after the SBF treatment, the materials have to be considered non bioactive. Furthermore, in-vitro studies allowed us to compare for different samples the relative kinetics of the bioactive response: the shorter the time required for the HA/HCA layer formation, the higher the bioactivity of the material. In order to monitor HA and/or HCA formation, XRPD patterns, SEM-EDS analysis and FTIR spectroscopy were obtained for the glass powders and ICP ~~has been~~ was performed on the SBF solutions at different incubation times.

**Figure 4** reports XRPD pattern after SBF soaking at different times.

-----  
(Please, insert here **Figure 4**)  
-----

All samples showed a broad band centered at around 22-23° ascribable to phospho-silicate gel glasses. In particular, for the SG873psAPTS sample (section b) after 4 days of soaking two weak diffraction peaks at 32° and 26° (2θ value) which could be assigned to the (211) and (002) HA reflections respectively (JCPDS PDF no. 74-0565 ref. PCPFWIN Version 2.3; JCPDS (Joint Committee on Powder Diffraction Standards), International Center for Diffraction Data, Swarthmore, PA, 2002), are clearly evident; increasing the soaking time, the intensity of these reflections increases. The sample without APTS calcined at high temperature (section a)) showed a similar behaviour; already after 1 day of SBF soaking two weak broad peaks at 32° and 26° (2θ value) are present. Moreover after 4 and 7 days the patterns showed the presence of a weak but well defined peak centered at ~30° (2θ value)

attributed to calcite (main reflection peak (104), JCPDS PDF no. 86-0174 ref. PCPFWIN Version 2.3; JCPDS (Joint Committee on Powder Diffraction Standards), International Center for Diffraction Data, Swarthmore, PA, 2002).

In the case of reference sample calcined at low temperature (section c) a very weak peak attributed to (211) HA reflection appeared only after 14 days of SBF soaking times; this is an index of the low bioactivity response of SG423 sample with respect to SG873 one. The presence of organic and nitrate residues deriving from the synthesis decreases the rate of glass bioactivity. Concerning the APTSxxSG glasses (sections d and e), already after 1 day of SBF soaking, in the case of APTS25SG423 and APTS50SG423 a broad peak at 32° was detected for both samples and it is due to (211) HA reflection; the (104) reflection, typical of calcite, was also revealed for both samples; it increases with the increasing of APTS content. A similar behaviour was detected in our previous work<sup>30</sup> where bioactive glasses obtained by melt-quenched technique were post-synthesis functionalized onto the surface with TEOS or APTS: the glasses functionalized with APTS after SBF soaking showed higher amount of calcite with respect to that functionalized with TEOS. The explanation is strictly related to the lower ability to form a silica-gel layer on APTS-containing glass surface. The low amount of silica-gel layer reduces its efficacy to interact with release  $\text{Ca}^{2+}$  cation and the subsequent high  $\text{Ca}^{2+}$  concentration in solution enables the separation of simple binary compound as  $\text{CaCO}_3$  (see Table 4) clearly identified after 1 day.

From these data it is possible to confirm that the presence of APTS in the glass structure does not inhibit the glass bioactivity. Section f of Figure 4 allows to monitor the rate of HA formation as a function of soaking time in SBF. It is possible to note that the rate of HA increases as a function of calcination temperature. Moreover, increasing the APTS content in the glass composition decreases the rate of HA formation.

The XRPD results were confirmed by SEM-EDS analysis of SG873, APTS25SG423 and APTS50SG423 after 14 days of SBF soaking. The morphology of samples were changed significantly, showing greater homogeneity with respect to the as synthesized samples shown in Figure 1.

In particular, for the SG873 and APTS25SG423 samples the glasses aggregates were covered by an external layer made up of new particles (see **Figure 5**, section A and B) whose morphology and composition (see Figure 5, section A' and B') is ascribable to the formation of an apatite-like phase.<sup>31</sup>

-----  
(Please, insert here **Figure 5**)  
-----

10 The morphology of the APTS25SG423 is quite different by the previous samples, in fact the dimension of aggregates is higher with a squarer shape, the EDS analysis were showed an higher concentration of calcium of this external layer formed by new particles suggesting the formation also of calcite. FTIR spectra carried out on the samples after different soaking times, for sake of brevity, are reported in the supplementary materials. (see **Figure 3 SM**) In the case of the SG873psAPTS sample  
15 (Section B of Figure 3 SM), the glass behaviour is similar to ~~what~~ that described in the case of SG873 sample (Section A of Figure 3 SM). According to **XRPD results**, the post-synthesis functionalization procedure does not influence the in-vitro bioactivity.

As previously reported in the **XRPD** section, concerning the samples calcined at low temperature and containing APTS, FTIR spectra confirm that the low calcination temperature decreases the rate of  
20 HA/HCA crystallization. For sake of brevity, FTIR spectra are reported in the supplementary materials. (see Figure 4 SM) In order to monitor the ions release **Table 4** reported ICP-ES data after the different soaking times in SBF of all the APTS-containing samples.

-----  
(Please, insert here **Table 4**)  
-----

The Si, Ca and P release is related to the amount of APTS used in the synthesis procedure; in fact, the APTS100SG423 was not characterized after the SBF soaking because it was completely dissolved in solution as confirmed by ICP analysis. In particular, the Si release can be directly related to the amount of APTS inserted during the synthesis; increasing the amount of APTS the Si release increases; increasing the APTS content there is a decrease in the silica reticulation and as a consequence a fast Si release in solution. The amount of Ca ions released by APTS25SG423 and APTS50SG423 samples was higher with respect to SG873psAPTS and SG873<sup>20</sup> samples, this is probably due to the Calcium ions that do not enter completely to the silica network until a temperature of >400°C (Lin et al J Mater Chem 2009).

However, it is possible to conclude that the presence of low amounts of APTS (APTS25SG423 and APTS50SG423 samples) in the glass structure does not inhibit the HA/HCA crystallization, although the APTS delays the HA/HCA crystallization rate. The APTS-containing glasses maintain the bioactivity with the exception of APTS100SG423.

Moreover, the pH of SBF solution was monitored in order to control the effect of introduction of -NH<sub>2</sub> groups on the material surface. The pH values were reported in Table 5.

-----  
(please, insert here Table 5)  
-----

The introduction of -NH<sub>2</sub> groups in APTS<sub>xxx</sub>SG<sub>yyy</sub> sample does not modify the pH values of SBF solutions; the main difference between the samples (with or without -NH<sub>2</sub> groups) was an initial increase of pH value due probably to the basicity of -NH<sub>2</sub> groups, whereas for the sample without -NH<sub>2</sub> groups the pH decreases until 4 hours of reaction as previously reported in ref. Aina et al.<sup>20</sup> After 7 days the pH was in the 7.14 - 7.38 range for both samples.

It is possible to conclude that, the behaviour of these new APTS-containing glasses in SBF was consistent with that of other bioactive glasses, due to their ability to develop an apatite-like layer onto

the surface when in contact with the simulated biological fluids. Further studies including cell-based tests and pre-clinical implantation studies would be required before they could be classed as bioactive glasses. Moreover exploiting the presence of  $-NH_2$  groups firmly anchored onto the glasses surface, it is possible to functionalize these materials by means of covalent bonds to graft organic spacers and/or biological molecules (drugs and/or proteins).

*Post-synthesis organic functionalization.* In order to evaluate a “smart” release of drugs anchored onto the glass surface a covalent functionalization on the APTS25SG423 glass with organic spacers, as previously described (see material section) has been performed. Moreover, pH-controlled release on the APTS25SG423-MA conjugates with cysteamine and 5-aminofluorescein was performed.

In **Figure 6** Raman spectra carried out on the APTS25SG423 samples after the covalent functionalization with the two organic spacers (maleic and cis-aconitic anhydrides) are reported.

-----

(please, insert here **Figure 6**)

-----

By the inspection of Raman spectra the following features can be evidenced:

*i)* the bands at  $\sim 2960$ ,  $\sim 2940$  and  $\sim 2890$   $cm^{-1}$  typical of asymmetric and symmetric C-H stretching vibrations are clearly detectable in all samples; these bands are due to the presence of both APTS and anhydrides molecules. The intensity ratio of these bands changed after the functionalization with the anhydrides with respect to APTS25SG423 glass;

*ii)* the bands at  $\sim 1850$   $cm^{-1}$  are due to stretching vibrations typical of carbonyl groups in the  $\alpha,\beta$ -unsaturated five-membered cyclic anhydrides. These bands are no longer present in the spectra due to the anhydrides' ring opening;

*iii)* the bands at  $\sim 1650$  and  $\sim 1600$   $cm^{-1}$  are due to ~~carboxyl~~ carbonyl groups stretching vibrations typical of carboxylic acid and amide, respectively. These bands appear on the glass after the covalent functionalization with the two anhydrides: the band at  $1600$   $cm^{-1}$  is a clear indication of the formation

of an amide bond between the  $\text{-NH}_2$  groups present on the glass surface and the carbonyl group of the anhydrides whereas the band at  $1650\text{ cm}^{-1}$  is typical of  $\text{C=O}$  stretching vibration of carboxylic groups resulting from the anhydrides' ring opening;

*iv*) in the  $1450\text{-}1200\text{ cm}^{-1}$  spectral range there are the characteristic bands of C-H bending modes;

*v*) the sharp band at  $\sim 1040\text{ cm}^{-1}$  as previously mentioned is typical of carbonate species.

Raman spectra confirm the efficiency of the covalent functionalization with the two anhydrides; indeed this reaction does not modify the glass matrix. Both anhydrides are covalently bonded at the glasses surface through the formation of an amide bond between the surface amino groups of the glass and the carbonyl groups of the anhydrides.

~~model molecules to simulate a drug containing an amino group; the  $\text{NH}_2$  functionality which Cysteamine possesses an amino group that~~ can form an amide bond with the free carboxylic ~~one~~ group on the glass surface deriving from the anhydrides' ring opening. ~~In the case of cysteamine, the group that~~ can form an amide bond with the free carboxylic one on the glass surface deriving from anhydrides. ~~In the case of cysteamine, the~~ presence of thiol groups allows to determine ~~from a quantitative point of view~~ by means of elemental analysis the ~~amount~~ presence of cysteamine ~~present onto the glasses surface before and after the release in the buffered solutions;~~ concerning the 5-aminofluorescein conjugate, due to its high molar extinction coefficient it was also possible to determine quantitatively the amount of fluorescein derivative released.

In **Figure 7** the evolution of weight % of N, C, H and S after different functionalization steps is reported.

-----  
(please, insert here **Figure 7**)  
-----

The theoretical amount of C and N in the APTS25SG423 sample should be 3.8 and 10.0% for N and C, respectively. It was possible to see that the experimental amount of N% was higher with respect to

the theoretical one: this can be explained by the presence of nitrate residues as yet reported in the discussion of thermal analysis results; concerning the C% content, it is slightly lower with respect to the theoretical one, this can be due to a partial decomposition of the aliphatic chain of the APTS molecules not well linked with the silica matrix that can occur during the calcinations at 423K. The functionalization of the glass with maleic (MA) anhydride did not modify the % of C, N and H, whereas the conjugation with the cysteamine molecules caused the increment of %S and the conjugation with 5-aminofluorescein which has a higher molecular weight resulted in an increment of %C and %H.

This is a very good result highlighting the ability of functional groups present on the material surface to be conjugated with molecules of biological interest. Moreover, concerning the cysteamine conjugate, it is interesting to note that the atomic ratio between N and S (N/S) is 2.9 (the theoretical one is 2); taking into account the presence of nitrate residues, it is in agreement with the functionalization scheme (see scheme 1 and 2).

In Figure 8 Raman spectra, in the 3100-500  $\text{cm}^{-1}$  range, carried out onto the samples after the different functionalization steps are reported.

-----  
(Please, insert here Figure 8)  
-----

Spectra (a) and (b) were described in the previous paragraph; concerning the spectrum of the sample functionalized with cysteamine (see spectrum (d)) it is possible to single out two main spectral features ascribable to the presence of cysteamine that are: i) the band at  $\sim 2925 \text{ cm}^{-1}$  typical of C-H stretching vibrations of cysteamine and a band located at  $\sim 675 \text{ cm}^{-1}$  ascribable to a C-S stretching vibration. Both these bands are present in the spectrum of pure cysteamine (see spectrum (D)). By the inspection of the amide bond spectral region ( $1700\text{-}1600 \text{ cm}^{-1}$ ) it is possible to note that after the functionalization with cysteamine the intensity of the band at  $\sim 1600 \text{ cm}^{-1}$  increases and the band at  $\sim 1650 \text{ cm}^{-1}$  decreases.

This is an indication that there is the formation of other amide bonds. The persistence of the –COOH band suggests that the reaction between the -NH<sub>2</sub> groups of cysteamine and the carboxylic groups present onto the **functionalized** glass surface is not complete, nevertheless, due to the glass degradation in the reaction conditions, it was not possible to modify the functionalization conditions.

5 Concerning the conjugation with 5-aminofluorescein spectra of APTS25SG423-MA-AF sample conjugated with 5-aminofluorescein (spectrum e) and of pure 5-aminofluorescein, (spectrum E) as reference are reported in Figure 9. After the conjugation reaction with 5-aminofluorescein it is possible to single out the bands in the 1450-1200 cm<sup>-1</sup> spectral range, characteristic of C-H bending modes of 5-AF, moreover the bands at ~ 1650 and 1600 cm<sup>-1</sup> typical of amide bond are detectable. Raman spectra  
10 confirm the efficiency of the covalent functionalization with both cysteamine and 5-aminofluorescein with the formation of an amide bond between the anhydride and the amino groups of both cysteamine or 5-AF.

In **Figure 9** the Raman spectra of the sample functionalized with cysteamine after the different releasing times (1 and 72 hours) in two different buffered solutions (PBS pH = 7.4 and acetate pH =  
15 4.5) are reported.

-----  
(please, insert here **Figure 9**)  
-----

~~It is possible to evaluate the~~ The release of cysteamine as a function of the pH has been monitored by  
20 means of Raman spectroscopy from a qualitative point of view. As previously mentioned, the insertion of the organic spacer (maleic anhydride) has the aim to obtain a pH sensitive amide bond able to release the drug only at acid pH. By the inspection of the spectra reported in Figure 9 it is possible to note that there are no appreciable differences between the samples reacted for 1 hour in the two buffered solutions (see spectra (d 1h PBS) and (d 1h Ac)). On the contrary after 72 hours of releasing  
25 time in the case of the sample reacted in acetate buffer (pH = 4.5)-(see spectrum d 72h Ac) there is no

evidence of cysteamine onto the glasses surface whereas in the case of the sample reacted 72 hours in PBS solution (pH = 7.4) (see spectrum d 72h PBS) it is possible to single out the presence of both amide and carboxylic bands (1650 and 1600  $\text{cm}^{-1}$ ). ~~With this preliminary delivery test (qualitative data) it has been demonstrated that a pH-sensitive drug delivery system has been developed.~~ The qualitative data obtained from the material characterization and delivery tests are in accordance with the formation of a covalent bond which can be hydrolyzed in acidic conditions.

The quantitative data concerning the release of 5-aminofluorescein by means of fluorescence spectroscopy are reported in **Figure 10**.

-----

(please, insert here **Figure 10**)

-----

The release of 5-AF presents a time-dependent trend: with longer soaking times, the amount of 5-AF released from both buffered solutions increases. This datum confirms the ability of these materials to act as controlled drug delivery system. Indeed, comparing the release at two different pH, it is possible to note that at pH 4.5 the amount of 5-AF released is higher than at pH 7.4, this evidence demonstrated that the amount of 5-AF released is higher at acid pH with respect to physiological one which is consistent with the development of a pH-sensitive drug delivery system.

The percentage of 5-AF released after 7 days is less than 1%. Despite the low solubility of 5-AF and considering the very low  $\text{IC}_{50}$  for doxorubicin, the therapeutic effects can be achieved even with the low amount released from our system where the drug would be delivered directly in the tumour site.

These preliminary data are indeed promising results in view of the development of a pH-sensitive drug delivery system. As future perspective doxorubicin, an anticancer drug containing amino groups in the structure, will be used instead of cysteamine or aminofluorescein and a complete more detailed release kinetics, at different times, in the buffered solutions at different pH, will be performed by means of UV-Vis and fluorescence spectroscopies.

## CONCLUSIONS

In this work, through an accurate **synthetic synthesis** approach and using different characterization techniques it was possible **to** prepare a new functionalized bioactive glass. As mentioned in the results and discussion section, compared to the post-synthesis functionalization with APTS, this glass **possesses** higher amount of amino groups which are firmly anchored onto the surface. These functionalities are available for conjugation with suitable molecules. For the first time the bioactivity properties of a gel glass are combined with the development of a pH-sensitive system able to release molecules of biological interest. In particular, among the synthesized materials, the APTS25**BSG**423 glass showed bioactivity in SBF after 4 days of soaking with the formation of an **apatite-like** layer onto **the** surface. Moreover, this glass has been covalently modified with organic molecules (**functionalization with** maleic or cis-aconitic anhydrides and **conjugation with** cysteamine and **5-aminofluorescein**) showing a total release **from the conjugates of cysteamine** only in conditions of acid pH (4.5) whereas at physiological pH (7.4) in conditions close to neutrality a slow release of this organic molecules **has** been observed.

**~~In this way,~~** Our work must be viewed as the first step in the development of a bioactive biomaterial functionalized with organic molecules and also able to release them only at acid pH **~~has been successfully developed.~~** This **preliminary** work opens the door to the synthesis **of a series** of bioactive glasses to be used not only as bone fillers but also as “smart drug delivery systems responsive to specific-stimuli”.

## ACKNOWLEDGEMENT

The authors acknowledge Dr. C. Giovannoli of University of Torino for acid-basic titration measurements, Prof. E. Diana of University of Torino for Raman measurements.

V.A., G.C. and G.M. acknowledge Compagnia di San Paolo for the financial support (Project: ORTO11RRT5).

G.L. acknowledges Fondazione di Vignola for the financial support (Progetto “Materiali per la teranostica: progettazione di sistemi contenenti nanoparticelle e molecole di interesse biologico”).

---

## REFERENCES

- (1) Arcos, D.; Vallet-Regi, M. Bioceramics for drug delivery. *Acta Biomat.* **2013**, 61, 890-911.
- (2) Martina, M.; Subramanyam, G.; Weaver, J.C.; Hutmacher, D.W.; Morse, D.E.; Valiyaveetil, S. Developing macroporous bicontinuous materials as scaffolds for tissue engineering. *Biomaterials* **2005**, 26, 5609-5616.
- (3) Hench, L.L. Sol-gel materials for bioceramic applications. *Curr. Op. in Solid State and Mat. Sci.* **1997**, 2, 604-610.
- (4) Vitale-Brovarone, C.; Di Nunzio, S.; Bretcanu, O.; Verne, E. Macroporous glass-ceramic materials with bioactive properties. *J. Mat. Sci-Mat. in Med.* **2004**, 15, 209-217.
- (5) Caldorera-Moore, M.; Peppas, N.A. Micro- and nanotechnologies for intelligent and responsive biomaterial-based medical systems. *Adv. Drug Del. Rev.* **2009**, 61, 1391-1401.
- (6) McCoy, C.P.; Brady, C.; Cowley, J.F.; McGlinchey, S.M.; McGoldrick, N.; Kinnear, D.J.; Andrews, G.P.; Jones, D.S. Triggered drug delivery from biomaterials. *Exp. Op. on Drug Del.* **2010**, 7, 605-616.
- (7) Takahashi, Y.; Yamamoto, M.; Tabata, Y. Enhanced osteoinduction by controlled release of bone morphogenetic protein-2 from biodegradable sponge composed of gelatin and beta-tricalcium phosphate. *Biomaterials* **2005**, 26, 4856-4865.
- (8) Langer, R.; Peppas, N.A. Advances in biomaterials, drug delivery, and bio-nanotechnology. *Aiche J.* **2003**, 49, 2990-3006.
- (9) Peppas, N.A.; Hilt, J.Z.; Khademhosseini, A.; Langer, R. Hydrogels in biology and medicine: From molecular principles to bionanotechnology. *Adv. Mat.* **2006**, 18, 1345-1360.
- (10) Gao, W.; Chan, J.M.; Farokhzad, O.C. pH-Responsive Nanoparticles for Drug Delivery. *Mol. Pharm.* **2010**, 7, 1913-1920.
- (11) Pardoe, H.; Clark, P.R.; St Pierre, T.G.; Moroz, P.; Jones, S.K. A magnetic resonance imaging based method for measurement of tissue iron concentration in liver arterially embolized with ferrimagnetic particles designed for magnetic hyperthermia treatment of tumors. *Mag. Res. Im.* **2003**, 21, 483-488.
- (12) Needham, D.; Anyarambhatla, G.; Kong, G.; Dewhirst, M.W. A new temperature-sensitive liposome for use with mild hyperthermia: Characterization and testing in a human tumor xenograft model. *Cancer Res.* **2000**, 60, 1197-1201.
- (13) Rapoport, N. Combined cancer therapy by micellar-encapsulated drug and ultrasound. *Int. J. Pharm.* **2004**, 277, 155-162.

- (14) Kataoka, K.; Matsumoto, T.; Yokoyama, M.; Okano, T.; Sakurai, Y.; Fukushima, S.; Okamoto, K.; Kwon, G.S. Doxorubicin-loaded poly(ethylene glycol)-poly(beta-benzyl-L-aspartate) copolymer micelles: their pharmaceutical characteristics and biological significance. *J. Controlled Rel.* **2000**, *64*, 143-153.
- 5 (15) Park, J.W. Liposome-based drug delivery in breast cancer treatment. *Breast Cancer Res.* **2002**, *4*, 93-97.
- (16) Verne, E.; Vitale-Brovarone, C.; Bui, E.; Bianchi, C.L.; Boccaccini, A.R. Surface functionalization of bioactive glasses. *J. Biomed. Mat. Res. Part A* **2009**, *90A*, 981-992.
- (17) Manzano, M.; Vallet-Regi, M. Revisiting bioceramics: Bone regenerative and local drug delivery  
10 systems. *Prog in Sol State Chem.* **2012**, *40*, 17-30.
- (18) Branda, F.; Silvestri, B.; Luciani, G.; Costantini A. The effect of mixing alkoxides on the Stöber particles size. *Colloids and Surfaces- A: Physico-Chem. Eng. Aspect.* **2007**, *299*, 252- 255.
- (19) Zhang, H.; Li, F.; Yi, J.; Cu, C.; Fan, L.; Qiao, Y.; Tao, Y.; Cheng, C.; Wu, H. Folate-decorated maleilated pullulan-doxorubicin conjugate for active tumor-targeted drug delivery. *Europ J Pharm Sci.*  
15 **2011**, *42*, 517-26.
- (20) Aina, V.; Morterra, C.; Lusvardi, G.; Malavasi, G.; Menabue, L.; Shruti, S.; Bianchi, C.L.; Bolis, V. Ga-Modified (Si-Ca-P) Sol-Gel Glasses: Possible Relationships between Surface Chemical Properties and Bioactivity. *J. Phys.Chem. C.* **2011**, *115*, 22461-22474.
- (21) Lusvardi, G.; Malavasi, G.; Aina, V.; Bertinetti, L.; Cerrato, G.; Magnacca, G.; Morterra, C.;  
20 Menabue, L. Bioactive Glasses Containing Au Nanoparticles. Effect of Calcination Temperature on Structure, Morphology, and Surface Properties. *Langmuir.* **2010**, *26*, 10303-10314.
- (22) Shen, W,C.; Ryser, H.J. Cis-Aconityl spacer between daunomycin and macromolecular carriers: a model of pH-sensitive linkage releasing drug from a lysosomotropic conjugate. *Biochem and Biophys Res Comm.* **1981**, *102*, 1048-1054.
- 25 (23) Ulbrich, K.; Subr, V. Polymeric anticancer drugs with pH-controlled activation. *Adv. Drug Del. Rev.* **2004**, *56*, 1023-1050.
- (24) Gupta, G.; Wagh, S.B. Synthesis and antifungal activity of N-(alkyl/aryl)-2-(3-oxo-1,4-benzothiazin-2-yl)acetamide. *Indian J. Chem. B* **2006**, *45*, 697-702.
- (25) Brunauer, S.; Emmet, P.H.; Teller, E.J. Adsorption of gases in multimolecular layers. *J. Am.*  
30 *Chem. Soc.* **1938**, *60*, 309-320.
- (26) Barrett, E.P.; Joyner, L.S.; Halenda, P.P. The Determination of Pore Volume and Area Distributions in Porous Substances. I. Computations from Nitrogen Isotherms. *J. Am. Chem. Soc.* **1951**, *73*, 373-380.

(27) Lippens, B.C.; de Boer, J.H. Studies on pore systems in catalysts : V. The t method. *J. Catal.* **1965**, 4, 319-331.

(28) Gregg, S.J.; Sing, K.S.W. Adsorption, Surface Area and Porosity: 2<sup>nd</sup> Edition. *San Diego,CA. Academic Press* **1995**.

5 (29) Kokubo, T.; Takadama, H. How useful is SBF in predicting in vivo bone bioactivity? *Biomaterials* **2006**, 27, 2907-2915.

(30) Shruti, S. Malavasi, G.; Lusvardi, G.; Menabue, L. Gallium-Containing Phosphosilicate Glasses: Functionalization and in-vitro Bioactivity. *Mat. Sci. Eng. C* **2013**, 33, 3190-3196.

(31) Franchini, M.; Lusvardi, G.; Malavasi G.; Menabue, L. Gallium-containing phospho silicate  
10 glasses: Synthesis and in vitro bioactivity. *Mat. Sci Eng. C* 2012, 32, 1401-1406.

## FIGURES

**Figure 1.** SEM micrographs of the as-synthesized samples: Reference glass (SG873 and samples with increasing amounts of APTS inserted during the synthesis procedure (APTS25SG423, APTS50SG423 and APTS100SG423, Sections A, B, C and D respectively).

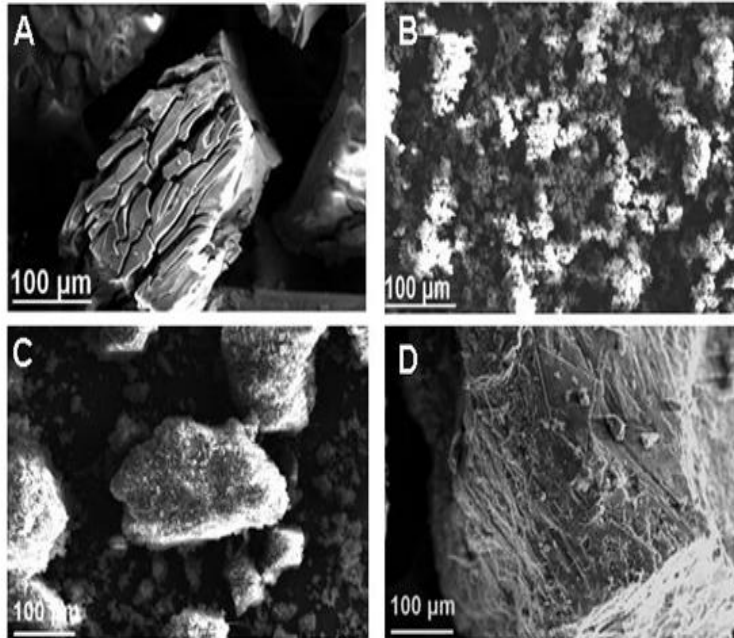


**Figure 2.** Thermo gravimetric analyses (TGA). In Section A data are reported as percentage of weight loss vs. temperature ( **temperature range 323 – 1100 K °C**) and in Section B data are reported as weight derivative (**%/K°C**) vs. temperature (**K °C**). (A) SG873, (B) SG873psAPTS; (a) SG423, (b) APTS25SG423, (c) APTS50SG423 and (d) APTS100SG423.

5



**Figure 3.** Raman spectra carried out on as-synthesized samples: (A) SG873, (B) SG873psAPTS; (a) SG423, (b) APTS25SG423, (c) APTS50SG423, (d) APTS100SG423 and (1) pure APTS as reference spectrum. Raman spectra, reported in the 3200-400  $\text{cm}^{-1}$  spectral range, are collected on powders in air.



**Figure 4.** XRPD patterns of SG873 (Section a), SG873psAPTS (Section b), SG423 (Section c), APTS25SG423 (Section d), APTS50SG423 (Section e) samples after 1 day (a), 4 days (b), 7 days (c) and 14 days (d) of SBF soaking. Section f reports for all samples the normalized counts of HA as a function of soaking time.

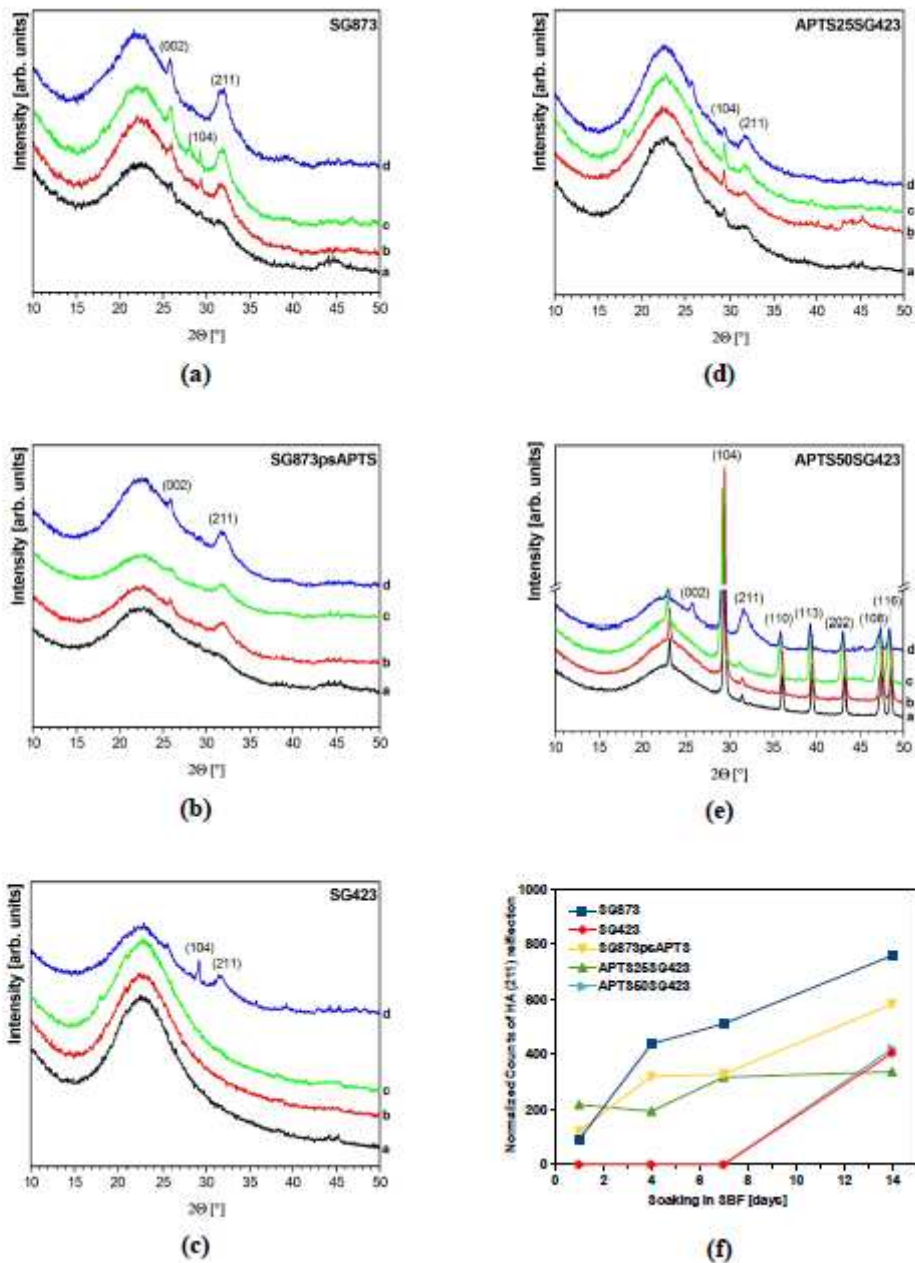


**Figure 5.** SEM micrographs of the samples as synthesized and after 14 days of SBF soaking: (A and A') SG873, (B and B') APTS25SG423 and (C and C') APTS50SG423 samples. In the section (A''), (B'') and (C'') the EDS spectra for the each sample after 14 days of SBF soaking are reported.

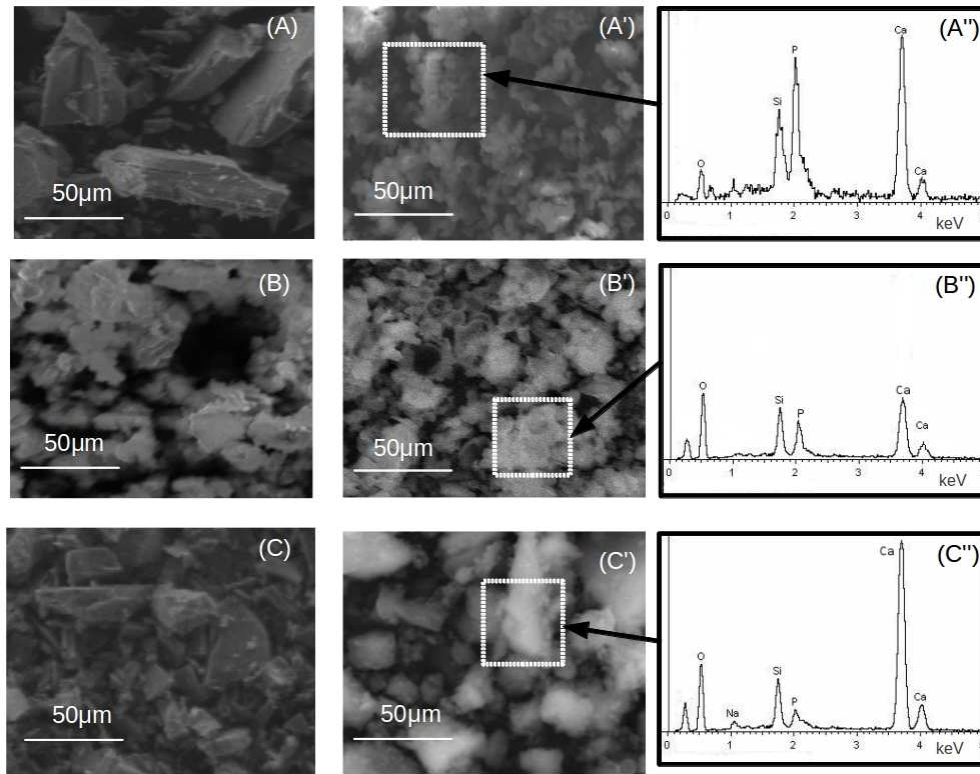


**Figure 6.** Raman spectra on as-synthesized samples: (a) APTS25SG423 and after functionalization with maleic (b) and cis-aconitic (c) anhydrides; as reference the spectra of pure maleic and cis-aconitic anhydrides are reported (see spectra B and C, respectively). Raman spectra are reported in the 3100-650  $\text{cm}^{-1}$  spectral range.

5

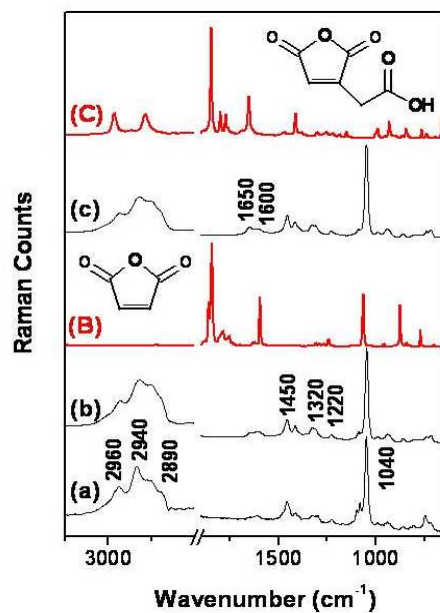


**Figure 7.** Weight % of N, C, H and S after different functionalization steps. The accuracy of elemental analysis data is ~ 2%.

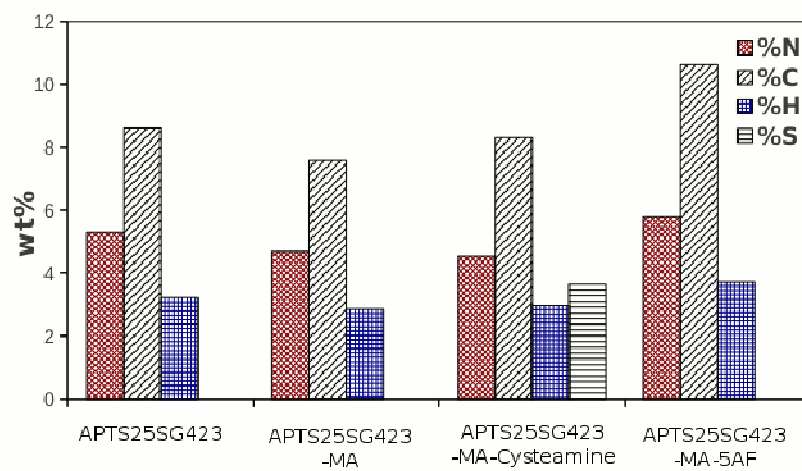


**Figure 8.** Raman spectra in the 3100-500  $\text{cm}^{-1}$  spectral range of (a) APTS25SG423 (b) APTS25SG423-MA sample functionalized with maleic anhydride (d) APTS25SG423-MA-CYST sample functionalized with maleic anhydride and cysteamine (D) pure cysteamine as reference spectrum (e) APTS25SG423-MA-AF sample functionalized with maleic anhydride and 5-aminofluorescein (E) pure 5-aminofluorescein as reference spectrum.

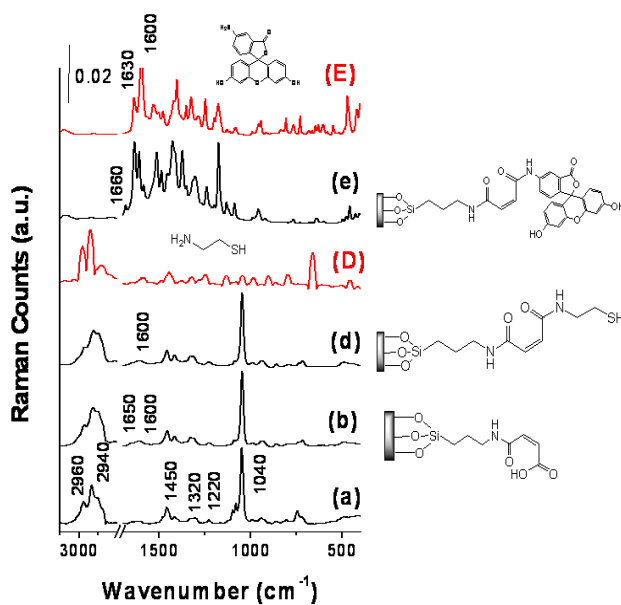
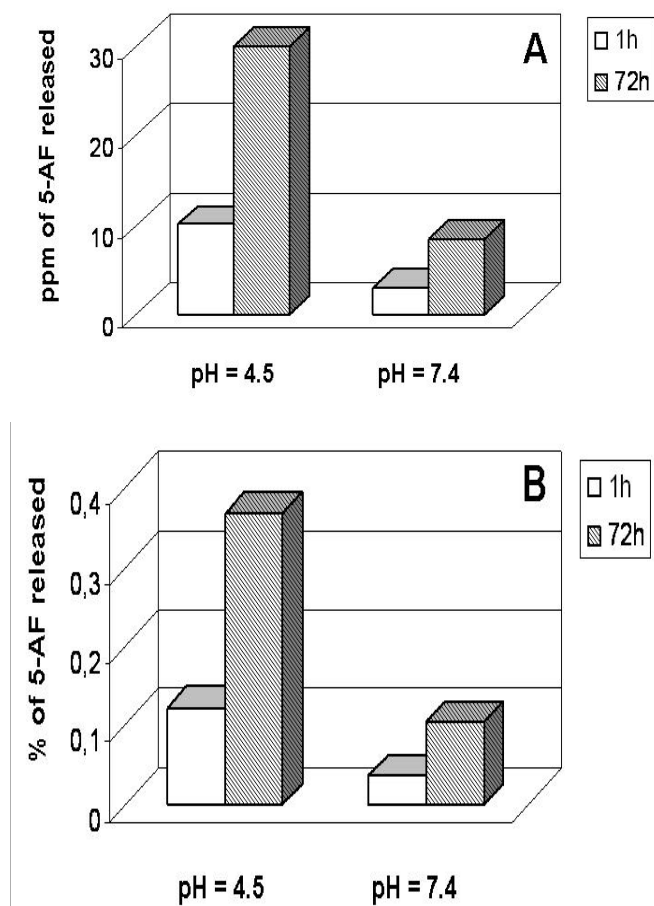


**Figure 9.** Raman spectra in the 1700-1300  $\text{cm}^{-1}$  spectral range of APTS25SG423-MA-CYST after 1 hour and 72 hours of reaction in PBS buffer at pH = 7.4 (d 1h PBS and d 72h PBS) and acetate buffer at pH = 4.5 (d 1h Ac and d 72h Ac).



**Figure 10.** Fluorescence data related to the amount of 5-aminofluorescein released are reported as ppm (Section A) and as percentage of 5-aminofluorescein released (Section B) in buffered solutions at pH 7.4 and 4.5 after 1 and 72 hours of reaction. The accuracy of elemental analysis data is ~ 5%.



**TABLES****Table 1.** Theoretical composition in molar % of studied glasses.

<b>Samples</b>		<b>SiO<sub>2</sub></b>		<b>CaO</b>	<b>P<sub>2</sub>O<sub>5</sub></b>	<b>Post-synthesis thermal treatment</b>
		<b>(% mol.)</b>		<b>(% mol.)</b>	<b>(% mol.)</b>	
		<b>TEOS</b>	<b>APTS</b>			
<b>Reference samples</b>	SG423	80	/			423K
	SG873	80	/	15	5	873K
<b>APTS samples</b>	SG873psAPTS	80		15	5	873K
	APTS25SG423	60	20	15	5	423K
	APTS50SG423	40	40	15	5	423K
	APTS100SG423	/	80	15	5	423K

**Table 2.** Experimental compositions expressed as oxides molar % for SG423, APTS25SG423 and APTS50SG423 were reported.

<b>Samples</b>		<b>SiO<sub>2</sub></b> (% mol.)	<b>CaO</b> (% mol.)	<b>P<sub>2</sub>O<sub>5</sub></b> (% mol.)
<b>Reference</b> <b>sample</b>	SG423	83.5 ±5.1	11.4 ±1.7	5.0 ±1.5
<b>APTS</b> <b>samples</b>	APTS25SG423	83.4 ±2.5	12.1 ±2.5	4.5 ±1.0
	APTS50SG423	82.9 ±2.8	12.3 ±1.8	4.8 ±1.2

**Table 3.** Specific surface area and porosity data of the as-prepared samples.

Samples		SSA (m <sup>2</sup> /g)		t-plot micropore area (m <sup>2</sup> /g)	BJH mesopore area (m <sup>2</sup> /g)	BJH mesopore width (Å)
		Kr	N <sub>2</sub>			
Reference samples	SG423		147 ± 7	/	120	26
	SG873		258 ± 15	95	125	26
APTS samples	SG873psAPTS		158 ± 18	/	58	14
	APTS25SG423		38 ± 2	/	/	/
	APTS50SG423	15 ± 1		/	/	/
	APTS100SG423	3.0 ± 0.3		/	/	/

**Table 4.** Concentration [ppm]\* of Si, Ca and P ( $\pm$  %std.dev) in the plain SBF solution and in the sample solution separated after different soaking times in SBF.

		Si [ppm] $\pm$ 5%	Ca [ppm] $\pm$ 8%	P [ppm] $\pm$ 5%
<b>SBF solution</b>	<i>t=0</i>	0	78	25
<b>SG873psAPTS</b>	1 day	58	76	26
	4 day	56	62	38
	7 days	64	92	36
	14 days	60	99	42
<b>APTS25SG423</b>	1 day	110	230	120
	4 day	122	205	107
	7 days	137	208	115
	14 days	155	250	150
<b>APTS505SG423</b>	1 day	450	120	190
	4 day	410	90	160
	7 days	440	110	220
	14 days	460	105	170
<b>APTS100SG423</b>	1 day	730	180	280
	4 day	800	200	310
	7 days	850	150	330
	14 days	1550	200	520

<sup>s</sup> Reported data are an average of three determinations on three independent-replica experiments.

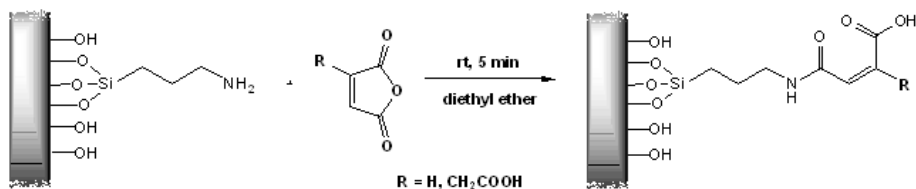
**Table 5.** pH of SBF solution to control the effect of introduction of -NH<sub>2</sub> groups on the material surface. The accuracy of elemental analysis data is ~ 5%.

<b>Soaking Times in SBF</b>	<b>Samples</b>			
	<b>SG873</b>	<b>SG423</b>	<b>APTS25SG423</b>	<b>APTS25SG423</b>
0	7.40	7.23	7.34	7.28
1 hour	7.35	7.24	7.40	7.80
2 hours	7.28	7.23	7.41	7.71
4 hours	7.12	7.16	7.43	7.50
8 hours	7.30	7.31	7.39	7.44
1 day	7.38	7.30	7.31	7.36
4 days	7.40	7.26	7.18	7.31
7 days	7.38	7.30	7.14	7.33

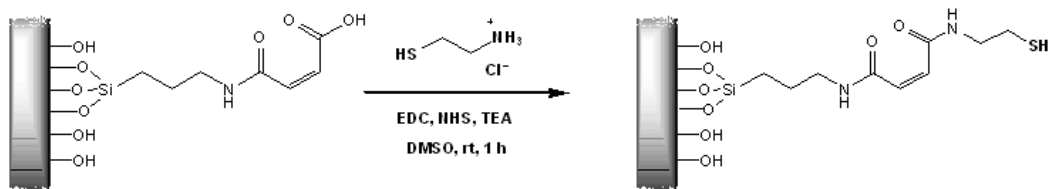
## SCHEMES

**Scheme 1:** Section A: **Synthetic Synthesis** procedure for the preparation of APTS25SG423-MA and APTS25SG423-CAA. Section B. Synthesis of the APTS25SG423-MA and cysteamine conjugate.  
5 Section C. Synthesis of the APTS25SG423-MA and 5-aminofluorescein conjugate.

### Section A



### Section B



### Section C

